# The Magnetic Field of the Solar Corona from Pulsar Observations

S. M. ORD[1], S. JOHNSTON[2], J. SARKISSIAN[3]
[1] *School of Physics, University of Sydney, Sydney, NSW 2006, Australia*
*(*steve.ord@gmail.com*)*
[2] *Australia Telescope National Facility, Epping NSW 1710, Australia*
[3] *Australia Telescope National Facility, Epping NSW 1710, Australia*

Received ; accepted

**Abstract.** We present a novel experiment with the capacity to independently measure both the electron density and the magnetic field of the solar corona. We achieve this through measurement of the excess Faraday rotation due to propagation of the polarised emission from a number of pulsars through the magnetic field of the solar corona. This method yields independent measures of the integrated electron density, via dispersion of the pulsed signal and the magnetic field, via the amount of Faraday rotation. In principle this allows the determination of the integrated magnetic field through the solar corona along many lines of sight without any assumptions regarding the electron density distribution. We present a detection of an increase in the rotation measure of the pulsar J1801−2304 of approximately 160 rad m$^{-2}$at an elongation of 0.95° from the centre of the solar disk. This corresponds to a lower limit of the magnetic field strength along this line of sight of $> 393\mu$G. The lack of precision in the integrated electron density measurement restricts this result to a limit, but application of coronal plasma models can further constrain this to approximately 20mG, along a path passing 2.5 solar radii from the solar limb. Which is consistent with predictions obtained using extensions to the Source Surface models published by Wilcox Solar Observatory

**Keywords:** Sun: magnetic field

## 1. Introduction

Our understanding of the solar corona is far from complete. Attempts are continually being made to marry theory and observations, but these efforts are hampered by the difficulty in obtaining direct measurements of physical properties throughout the corona. Without these measurements the state of the corona must be inferred from models that extrapolate from those observations that can be obtained from the solar surface or at distances comparable to 1 AU. Experiments have attempted to probe the outer corona via Faraday rotation through a variety of methods including measuring the rotation of the position angle of polarised emissions from the Cassini space probe (Jensen et al 2005) and Pioneer 6 (Levy et al 1969). Background radio sources have also been used to constrain the mean integrated line of sight magnetic field (Mancuso & Spangler 2000). We have used the co-axial 10/50cm receiver attached to the 64–m Parkes radio telescope to observe a

number of pulsars as the background radio sources. Pulsars have a number of advantages over the background sources observed successfully by Mancuso & Spangler (2005), pulsars are polarised point sources and the position angle (PA) of any linearly polarised component is routinely measured by pulsar observers, their radiation is also broadband and pulsed, allowing simultaneous observation at multiple frequencies and the direct determination of the electron density along the line of sight.

This method has been motivated by the success of the Cassini and background radio source experiments and can in principle present a unique opportunity to disentangle the two properties of the solar corona that contribute to any observed rotation measure (RM). Namely that by measuring the dispersion of the pulsar signal we can determine the coronal electron density independently, this allows the path integrated magnetic field to be uniquely determined without recourse to a theoretical model of the coronal density profile. Consequently we can determine whether any variations in observed RM are due to fluctuations in the field, or variations in electron density. This has not been possible in the previous experiments of this nature. A further motivation is the large number of simultaneous lines of sight through the corona that can be observed within a given session, therefore the 3-dimensional structure of the corona can be constrained to a considerable degree.

We carried out this experiment in 2006 December. We detected a large variation in rotation measure for one target, and smaller variations in the second target. No variation was detected in our calibrator pulsar, demonstrating the feasibility of the experiment and convincing us of the veracity of our results.

This paper is structured in the following manner, we firstly present the level of the effect we intend to measure, we determine this via a simple model magnetic field constructed from a potential field model using data from the Wilcox Solar Observatory and a model of the coronal electron density. We then discuss the details of the experimental method. We finally present the results of the experiment, together with the calibration observations

## 2. Experimental Justification

In order to explore the feasibility of this experiment we have constructed a relatively simple model solar corona, using a potential field model and separate electron density model. This construction was then used to examine the level of the expected variations in RM and DM.

## 2.1. The Potential Field Model

Many approaches to model the solar magnetic field have been taken; the earliest being the potential field model developed independently by Schatten et al. (1969) and Altschuler & Newkirk (1969). Which extends photospheric measurements from magnetograms out to a *source surface*, typically 2.5 $R_\odot$ from the centre of the sun. It is generally not considered wise to simply extrapolate from the field values at this surface out to arbitrary radii, as we have done here. This however, is not intended to be a perfect model of the field in the outer corona, but a general model that maintains the geometry of the field and provides approximate values for the field in a "typical" quiet sun.

Following Altschuler & Newkirk (1969), the potential field model begins with the assumption that the coronal field is supporting no currents is equivalent to:

$$\nabla \times \mathbf{B} = 0. \tag{1}$$

The magnetic field can therefore be represented as the negative gradient of the scalar potential, $\psi$,

$$\mathbf{B} = -\nabla\psi \tag{2}$$

Since

$$\nabla \cdot \mathbf{B} = 0, \tag{3}$$

then

$$\nabla \cdot \nabla\psi = 0, \tag{4}$$

which is equivalent to:

$$\nabla^2\psi = 0. \tag{5}$$

Therefore the potential satisfies Laplace's equation. A solution of Laplace's equation can be found in terms of Legendre polynomials. In this case we have used a series of Schmidt quasi-normalised Legendre polynomials. The potential field solution decomposed into spherical polar components, $r$, $\theta$, $\phi$, where $\theta$ is the co-latitude, is of the following form:

$$\begin{aligned} B_r &= \sum_{lm} P_l^m(\cos\theta)\left(g_{lm}\cos m\theta + h_{lm}\sin m\theta\right) \\ &\quad \times \left((l+1)\left(\frac{R_\odot}{r}\right)^{l+2} - l\left(\frac{r}{R_s}\right)^{l-1} c_l\right) \end{aligned} \tag{6}$$

$$\begin{aligned} B_\theta &= -1 \times \sum_{lm}\left(\left(\frac{R_\odot}{r}\right)^{l+2} + \left(\frac{r}{R_s}\right)^{l-1} c_l\right) \\ &\quad \times \left(g_{lm}\cos m\theta + h_{lm}\sin m\theta\right)\frac{\delta P_l^m(\cos\theta)}{\delta\theta} \end{aligned} \tag{7}$$

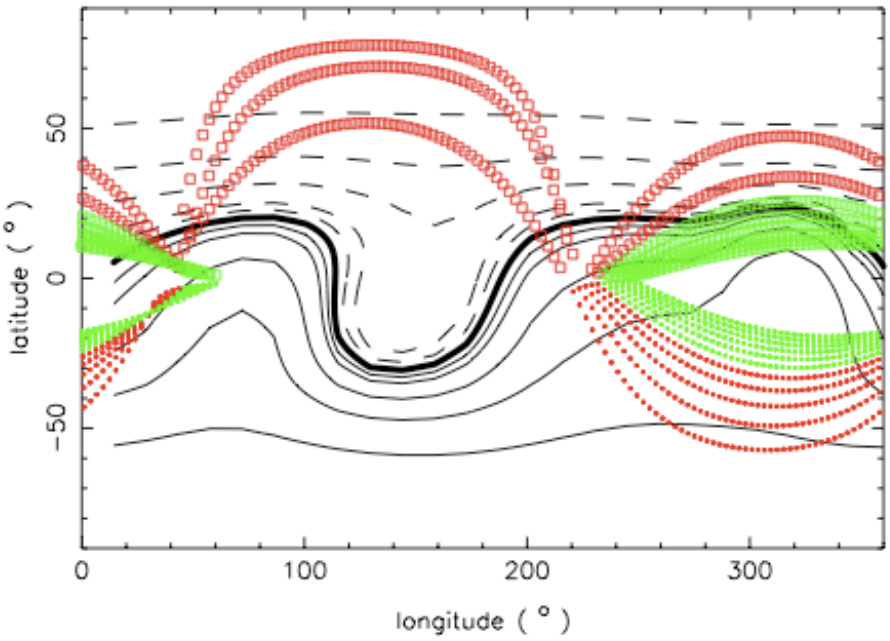


*Figure 1.* The radial component of the magnetic field of the sun at a distance of 2.5 solar radii from the centre of the sun. Calculated using the sum of Quasi-Schmidt Normalised Legendre polynomials. Using coefficients supplied by Wilcox Solar Observatory for Carrington rotation 2051. The contour lines are 0, ±1, 2, 5, 10, 20 $\mu$T, the solid black line being the neutral line. The boxes represent the lines of sight to J1801-2304, the dots are lines-of-sight to J1757-2421. The red symbols denote lines of sight between the 22nd and the 23rd of December, and the green symbols the 23rd and 24th.

$$B_\phi = \sum_{lm} \left( \left( \frac{R_\odot}{r} \right)^{l+2} + \left( \frac{r}{R_s} \right)^{l-1} c_l \right) \frac{m}{\sin\theta} \times (\cos\theta) \left( g_{lm} \sin m\theta - h_{lm} \cos m\theta \right) P_l^m(\cos\theta) \quad (8)$$

where:

$$c_l = -\frac{R_\odot}{R_s}, \quad (9)$$

$R_s$ is the distance to the source surface (2.5 $R_\odot$ in this case) and $R_\odot$ is the solar radius, the coefficients $h_{lm}$ and $g_{lm}$ are tabulated by Wilcox Solar Observatory for the rotation corresponding to the epoch of our experiment.

## 2.2. An Electron Density Model

We have applied the same electron model used by Mancuso & Spangler (2000). This is a two component model introduced by Guhathakurta et al.

(1996). The two components are a coronal hole and an equatorial streamer belt. The equatorial streamer confined to the region of zero magnetic field (the solid line in Figure 1).

The two components in the Mancuso and Spangler (2000) version of the Guhathukurta et al. (1996) model are designated $n_{CS}$ and $n_{CH}$, the *current sheet* and the *coronal hole*. They are combined in the following manner to obtain the total electron density, $w$ represents the width of the streamer and $\theta$ the angular distance in latitude above or below it:

$$\begin{aligned} n(r,\theta,\phi) &= n_{CH}(r) + [n_{CS}(r) - n_{CH}(r)] \\ &\quad \times \exp[-\theta^2/w^2(r,\phi)]. \end{aligned} \tag{10}$$

Where,

$$n_{CH}(r) = \left[16.15\left(\frac{r}{R_\odot}\right)^{-4.39} + 9.975\left(\frac{r}{R_\odot}\right)^{-4.09} + 1.099\left(\frac{r}{R_\odot}\right)^{-2}\right] \times 10^5. \tag{11}$$

and the streamer ($n_{CS}$) is given by:

$$n_{CS}(r) = \left[365\left(\frac{r}{R_\odot}\right)^{-4.31} + 3.6\left(\frac{r}{R_\odot}\right)^{-2}\right] \times 10^5, \tag{12}$$

the electron density being measured in $\mathrm{cm}^{-3}$. We have made the assumption in this model that the streamer is $\pi/16$ rad in width.

### 2.3. The Pulsars

The ecliptic plane is tilted with respect to the Galaxy, therefore at two times of the year the Sun passes through the Galactic plane as it is projected on the celestial sphere. The known pulsar population is preferentially distributed within the Galactic plane and interrogation of the ATNF pulsar database (Manchester et al. 2005) has provided a list of pulsars that pass close to the Sun (within 2.5 degrees) are grouped in ecliptic longitude and display appreciable flux in the frequency bands of interest. These pulsars are listed in Table I. We only attempted observations of a small subset of these pulsars, but they are all included in the table for completeness.

### 2.4. Pulsar Observations

Pulsars are point sources of periodic broad band noise. A pulsar observation consists of an integration, lasting typically hundreds or thousands of pulse periods, which is folded modulo the topocentric pulse period to obtain a pulse profile. Pulsar emission is in general polarised, but different pulsars display different degrees of circular and linear polarisation. The position

Table I. Possible Targets

| Pulsar Name | Ecliptic Longitude : Latitude | Flux (mJy) at 1400 MHz |
|---|---|---|
| J1652-2404 | 254.73 : -1.50 | 1.1[a] |
| J1721-2457 | 261.18 : -1.81 | unknown |
| J1730-2304 | 263.19 : 0.19 | 4[b] |
| J1733-2228 | 263.86 : 0.821 | 2.3[d] |
| J1753-2501 | 268.52 : -1.576 | 2.3[d] |
| J1756-2251 | 269.26 : 0.57 | 0.6[e] |
| J1756-2435 | 269.30 : -1.1554 | 2.0[d] |
| J1757-2421 | 269.42 : -0.9307 | 3.9[d] |
| J1757-2223 | 269.50 : 1.04 | 1.1[c] |
| J1759-2205 | 269.86 : 1.3467 | 1.3[d] |
| J1759-2302 | 269.96 : 0.40 | 1.3[c] |
| J1801-2304 | 270.31 : 0.36 | 2.2[d] |
| J1803-2137 | 270.89 : 1.8282 | 7.6[d] |
| J1807-2459A | 271.66 : -1.57 | 1.1[d] |
| J1817-2311 | 273.91 : 0.20 | unknown |
| J1822-2256 | 275.28 : 0.392 | 2.4[d] |
| J2048-1616 | 310.12 : 1.49 | 13[a] |

References:

a: Lorimer et al. (1995)

b: Kramer et al. (1998)

c: Morris et al. (2002)

d: Hobbs et al. (2004)

e: Faulkner et al. (2005)

angle of linear polarisation varies through the pulsar profile, but is stable in time.

Changes in the Faraday rotation that the radiation from pulsars is subjected to during passage through the solar corona manifests itself as a rotation of the polarisation angle of linear polarisation. This change in position angle is a function of frequency and is apparent both across the band and between observing bands. Changes in the electron content along the line of sight manifests itself as a dispersive delay between the arrival of the pulse at different frequencies.

2.4.1. *Measuring Dispersion and Rotation Measure*
In routine pulsar observations the ionised content of the interstellar medium (ISM) results in a dispersive delay between pulse arrival times at different frequencies. For this experiment there is a further delay due to the electron content in the solar corona. Although this is a small effect it is measurable if the same pulse can be observed over a considerable frequency interval. Measurement of this delay provides an independent measure of the electron content along the line of sight from the following relation:

$$\Delta t = \frac{e^2}{2\pi m_e c} \times \left(\frac{1}{f_1^2} - \frac{1}{f_2^2}\right) \times \int_0^d n_e \mathrm{d}l, \tag{13}$$

which is generally expressed as:

$$\Delta t \simeq 4.15 \times 10^6 \mathrm{ms} \times \left(\frac{1}{f_1^2} - \frac{1}{f_2^2}\right) \times \mathrm{DM} \tag{14}$$

where both frequencies are in MHz, and the dispersion measure (DM) is expressed in $\mathrm{cm}^{-3}\mathrm{pc}$.

The rotation measure (RM) is defined as:

$$\mathrm{RM} = \frac{e^3}{2\pi m_e^2 c^4} \times \int_0^d n_e \mathbf{B} \cdot \mathrm{d}\mathbf{l} \tag{15}$$

The total Faraday rotation is integrated along a path, and the total angular rotation in polarisation position angle being given by:

$$\Delta\Phi = \lambda^2 \times \mathrm{RM}, \tag{16}$$

It is readily appreciated that if both RM and DM can be measured then the integrated magnetic field strength along the path can be obtained via:

$$\langle \mathrm{B}_\parallel \rangle = 1.23\mu\mathrm{G} \left(\frac{RM}{\mathrm{rad\,m}^{-2}}\right) \left(\frac{DM}{\mathrm{cm}^{-3}\mathrm{pc}}\right)^{-1} \tag{17}$$

## 3. The Experiment

### 3.1. Observations

The observations were carried out using the Parkes radio telescope between 2006 December 20 and 28. Of the pulsars listed in Table 1 we observed PSRs J1801−2304, 1757−2421, 1757−2223 and J1822−2256. Of these, only the first two were useful for this experiment; the latter two had very low linear polarization and it was very difficult to measure an accurate RM. We

Table II. Results for PSR J1757−2421

| Date | Elongation (deg) | DM ($cm^{-3}pc$) | RM (rad $m^{-2}$) |
|---|---|---|---|
| Dec 20 | 1.89 | 179.5 ±0.12 | −33±2 |
| Dec 21[b] | 1.10 | 177.4±0.5 | −26±2 |
| Dec 22[a] | 1.11 | −− | −− |
| Dec 23 | 1.96 | 179.9±0.2 | −26±2 |
| Dec 24 | 2.88 | 179.8±0.2 | −26±2 |
| Dec 28 | 8.43 | 179.4±0.06 | −26±2 |

a: Not observed
b: Very weak

also observed a calibrator pulsar, PSR J1644−4559 whose properties are well known (Johnston 2004) and which is far enough away from the Sun to undergo no changes in its parameters.

We observed at 3 different wavebands, 50cm, 20cm and 10cm, using two different receiver packages. The first was the H-OH receiver at a central frequency of 1369 MHz with a bandwidth of 256 MHz. We also used the 10/50 cm receiver, a dual frequency system capable of observing simultaneously at both 650 and 3000 MHz. We used central frequencies of 3100 MHz with a bandwidth of 512 MHz and 690 MHz with an effective bandwidth (after interference rejection) of 35 MHz.

All receivers have orthogonal linear feeds and also have a pulsed calibration signal which can be injected at a position angle of 45 degrees to the two feed probes. A digital correlator was used which subdivided the bandwidth into 1024 frequency channels and provided all four Stokes' parameters. We also recorded 1024 phase bins per pulse period for each Stokes' parameter. The pulsars were observed for ∼30 minutes on each occasion and prior to the observation of the pulsar a 3-min observation of the pulsed calibration signal was made. The data were written to disk in FITS format for subsequent off-line analysis.

Data analysis was carried out using the PSRCHIVE software package (Hotan et al. 2004) and the analyis and calibration were carried out in an identical fashion in that described in detail in Johnston et al. (2005). Most importantly, we are able to determine absolute position angles (PA) for the linearly polarized radiation at all three of our observing frequencies.

Table III. Results for PSR J1801−2304

| Date | Elongation (deg) | DM ($cm^{-3}pc$) | RM (rad $m^{-2}$) |
|---|---|---|---|
| Dec 20 | 2.60 | 1071.9±0.4 | −1170±7 |
| Dec 21[a] | 1.50 | −− | −− |
| Dec 22[b] | 0.44 | −− | −− |
| Dec 23 | 0.96 | 1070.1±0.5 | −977±7 |
| Dec 24 | 1.84 | 1069.2±0.4 | −1145±7 |
| Dec 25 | 2.91 | 1070.0±0.3 | −1160±7 |
| Dec 27 | 5.11 | 1070.2±0.4 | −1158±7 |

a: Not observed
b: Very weak

### 3.2. Results

The absolute polarization calibration at all three observing frequencies allows us to obtain a more accurate RM in the following way. First we obtain the RM through fitting to the PAs of the linear radiation as a function of observing frequency across the band at a single frequency. We then improve the RMs by comparing PAs between the different frequency bands, where the large lever arm yields a much smaller error bar. Unfortunately, this is not possible for PSR J1801−2304 because the pulsar is essentially invisible at our lowest frequency. We therefore rely on the 3.1 GHz data to deduce the RM.

The dispersion measure (DM) was computed by first measuring the time of arrival of the pulsar as a function of frequency across the observing band. Then equation 14 was fitted in the arrival times to determine an accurate value of DM.

Results for PSRs J1757−2421 and J1801−2304 are shown in tables II and III respectively. There is a surprising difference between the two cases. For PSR J1757−2421, the RM of the pulsar far from the Sun is $-26\ \mathrm{rad\,m^{-2}}$ and we only see deviations from this value at a single epoch (Dec 20). For PSR J1801−2304 in contrast we see significant variations from day to day. The RM of the pulsar far from the Sun is $-1150\ \mathrm{rad\,m^{-2}}$ and this value was also obtained once the pulsar was more than 5 degrees from the Sun. However, on Dec 23, when the pulsar was less than 1 degree from the Sun's centre, we recorded an RM change of $160\ \mathrm{rad\,m^{-2}}$. On Dec 22, the date of the closest approach to the Sun, the total intensity of the pulsar was

low (likely caused by an increase in the system temperature because of the proximity to the Sun) and we were unable to determine an RM value.

This is an extremely high RM variation, although not unprecedented in the pulsar literature. PSR B1259−63 is in an eccentric orbit about a Be star companion (Johnston et al. 1992). During the periastron approach, the RM changes significantly, reaching a peak variation in excess of $10^4$ rad m$^{-2}$ (Conners et al. 2002; Johnston et al. 2005). The implications of this change are that the magnetic field in the vicinity of the Be star of ∼6 mG.

### 3.3. The Predictions

The simple models described in section 2 have been used to model this experiment. The line of sight to each pulsar as the Sun moves across the sky has been projected through the model solar corona and the change in measured electron content and excess Faraday rotation predicted as a function of observing day. Figure 2 presents the expected Faraday rotation at the three observing wavelengths. The predictions indicate that a large change in rotation measure for J1801−2304 was actually expected for the days in question. However the observed RM change is higher even than the prediction suggesting that our simple model is not fully describing the state of the magnetosphere. The predictions suggest that an even greater effect would have been observed around the 22nd of December, however as noted previously, observations taken on that day has a signal to noise ratio too low to detect a variation in RM.

#### 3.3.1. *Rotation Measure*

The modeling has revealed that the expected level of position angle rotation is incredibly variable, both as a function of observing day and ecliptic latitude. This is due to the geometry of the coronal magnetic field. If the line–of–sight to the pulsar projects through a symmetric coronal magnetic structure then the resultant RM will be negligible. However if the solar corona is asymmetric the RM, and thus the rotation in PA, can be considerable. Figure 2 shows this clearly; there is essentially no rotation in the PA except for one day within the two week period simulated in the Figure. The results are not unprecedented, Mancuso and Spangler (2000) indicate variable measured RM (from 0 to 11 rad m$^{-2}$) at a considerable distance from the Sun and Ingleby et al. (2007) detect an RM change of 61 rad m$^{-2}$ at a distance greater than 5 solar radii.

J1757−2421 also passes close to the solar limb, however it does not display significant excess Faraday rotation. The explanation is provided by Figure 3 which indicates that the expected Faraday rotation is very low. This is due to the line of sight traversing a generally symmetric field configuration, which can be discerned from Figure 1.

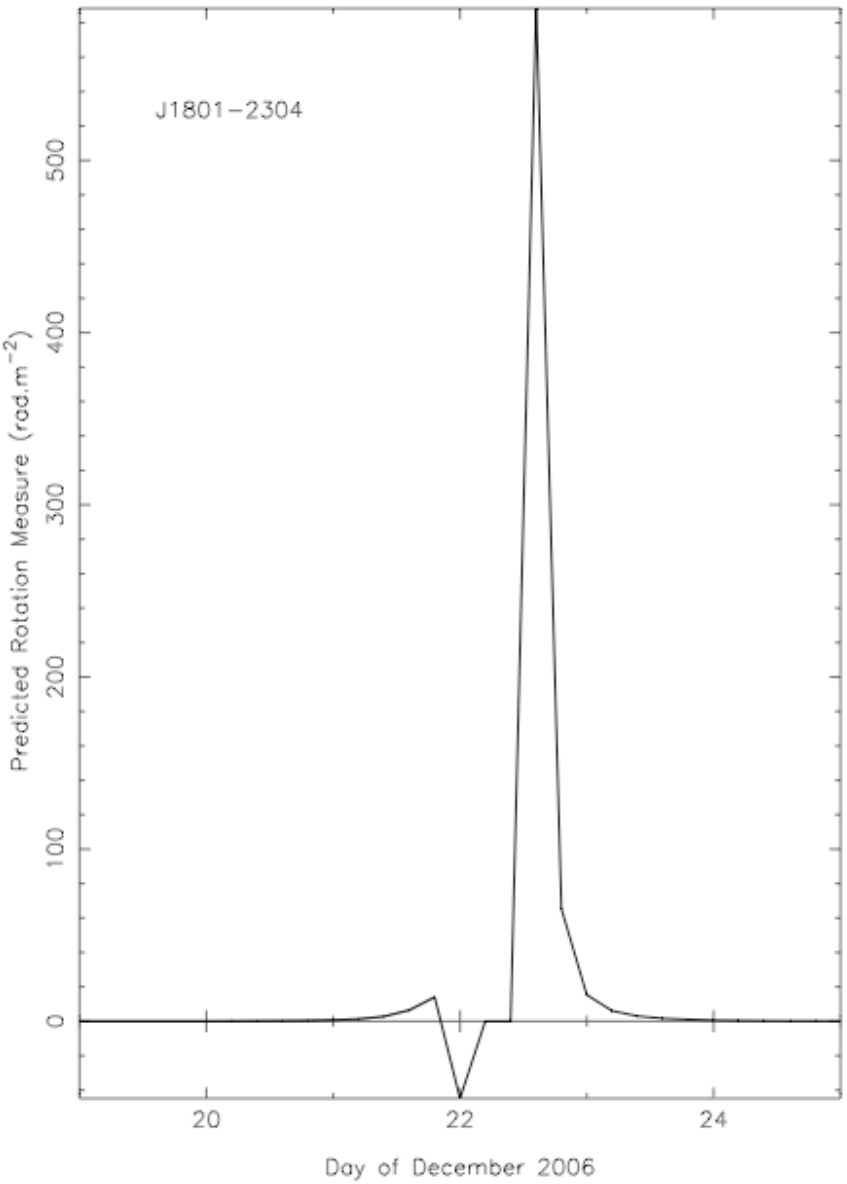


*Figure 2.* The predicted excess Faraday rotation for J1801−2304. The pulsar was observed throughout this period, unfortunately the observation at the height of the predicted Faraday rotation has insufficient signal to noise ratio to allow a confirmation

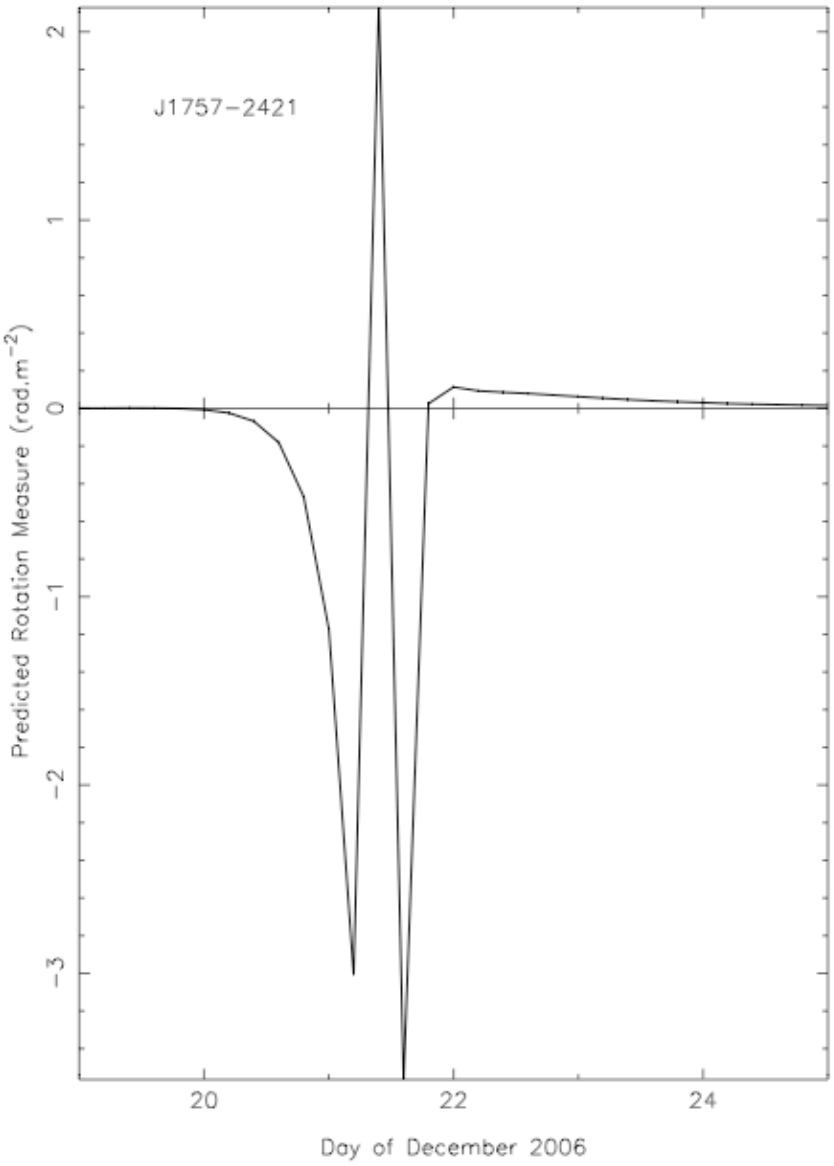


*Figure 3.* The predicted excess Faraday rotation for J1757−2421. The line of sight to this pulsar traverses regions of the corona that are symmetric in their magnetic field and electron properties, therefore it displays little net Faraday rotation.

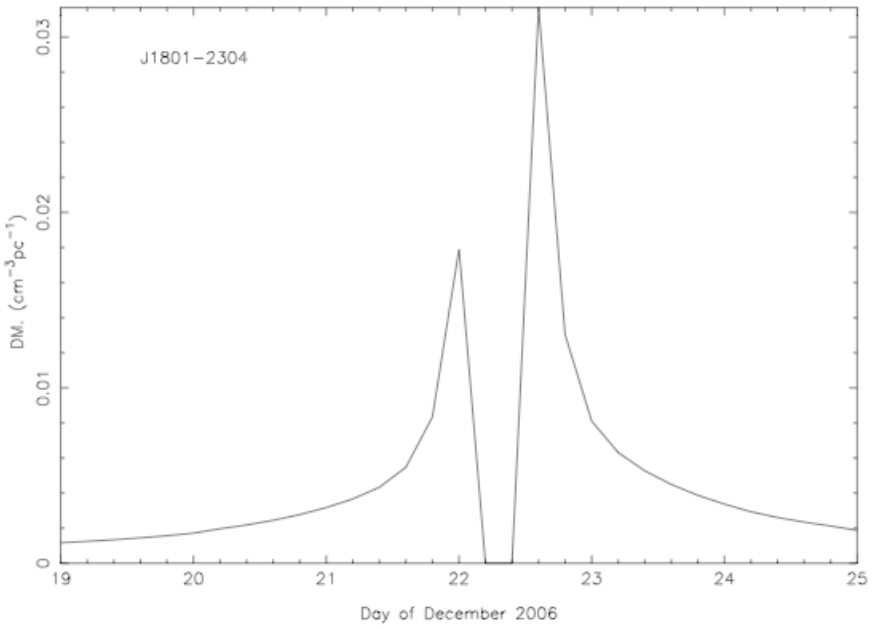


*Figure 4.* The expected DM variations for J1801−2304.

3.3.2. *Dispersion Measure*

The essential difference between this experiment and that performed by Mancuso and Spangler (2000), is that we are observing simple polarised point sources, with a single dish and that we can independently measure the electron component in the coronal plasma. Pulsar observations typically consider the solar wind as a source of an additional dispersive delay to that imposed upon observations by the Interstellar Medium. The analysis of pulse times–of–arrival typically attempt to remove the additional delay imposed by the solar wind by assuming a very simple model of the solar corona (see Lommen et al. 2006 for a discussion). This has long been considered a gross simplification by the pulsar community and work is currently underway to greatly improve upon the current model (Edwards et al. 2006) . Inadequacies in the current model have been apparent as periodic DM variations in timing observations of some pulsars for example Splaver et al. (2005) present a periodic DM variation of $2 \times 10^{-4}$ pc cm$^{-3}$ for the pulsar J1713+0747. Our predictions indicate a level of DM variation at 10 times this level (few $\times 10^{-3}$ pc cm$^{-3}$) for some objects, as presented in Figure 4. This will be challenging to measure for some of the pulsars in Table 1 as the arrival time precision is not high.

Changes in DM of order $10^{-3}$ pc cm$^{-3}$ require a timing precision of several $\mu$ s at both 10 cm and 50 cm simultaneously. Timing arrival precision is given, as a rough rule of thumb, by the width of the pulse divided by the signal–to–noise ratio of the observation. As most of the target list have widths of order 10 ms, high signal–to–noise ratios will be required to obtain the required measurement precision. However some of the target pulsars, notably the millisecond pulsars PSR J1730–2304 and PSR J1756–2251, have a pulse width of order 1 ms and such should allow sufficient measurement precision.

We were unable to detect any variation in dispersion measure for J1801−2304 due to a lack of such precision in time of arrival. Figure 4 indicates the expected level of DM variation and as can be seen from Table III our DM measurement accuracy falls a long way short.

### 3.4. Magnetic Field

The dispersion measure precision presented in Table III is 0.5 cm$^{-3}$pc, any DM contribution due to the plasma of the solar corona must be less than this. We can therefore use this limit to indicate a minimum magnetic field (using Equation 17) of $> 393\mu$G or 3.93nT. Under the assumption that the coronal plasma model outlined in § 2.2 and shown in Figure 4 is a reasonable representation of the coronal electron density, we can further constrain the integrated magnetic field. Assuming from Figure 4 the DM contribution on the December 23rd is approximately 0.01 cm$^{-3}$pc for the line of sight to J1801−2304 our RM measurement constrains the net integrated line of sight magnetic field to be approximately 20mG or $0.2\mu$T at an elongation of 0.96 degrees from the centre of the disk (2.7 solar radii from the solar limb).

## 4. Conclusion

We have presented details of an experiment with the potential to independently probe both the electron and magnetic field properties within the solar corona. We have proven the practicality of this experiment by presenting rotation measure variations detected as J1801−2304 passed close to the limb of the Sun. These RM measurements indicate a net magnetic field of $0.2\mu$T at 2.7 solar radii for the solar limb.

This experiment, if conducted in a more complete manner has the potential to independently map the coronal plasma density and magnetic field along multiple lines of sight. As such it is a useful contribution to the current experimental probes of coronal properties.

## References

Altschuler, M. D. & Newkirk, G. 1969, Solar Phys., 9, 131
Connors, T. W., Johnston, S., Manchester, R. N., & McConnell, D. 2002, MNRAS, 336, 1201
Edwards, R. T., Hobbs, G. B., & Manchester, R. N. 2006, MNRAS, 372, 1549
Faulkner, A. J., Kramer, M., Lyne, A. G., et al. 2005, ApJ, 618, L119
Guhathakurta, M., Holzer, T. E., & MacQueen, R. M. 1996, ApJ, 458, 817
Hobbs, G., Faulkner, A., Stairs, I. H., et al. 2004, MNRAS, 352, 1439
Hotan, A. W., van Straten, W., & Manchester, R. N. 2004, Proc. Astr. Soc. Aust., 21, 302
Ingleby, L. D., Spangler, S. R., & Whiting, C. A. 2007, ArXiv Astrophysics e-prints
Jensen, E. A., Bird, M. K., Asmar, S. W., et al. 2005, Advances in Space Research, 36, 1587
Johnston, S. 2004, MNRAS, 348, 1229
Johnston, S., Ball, L., Wang, N., & Manchester, R. N. 2005, MNRAS, 358, 1069
Johnston, S., Hobbs, G., Vigeland, S., et al. 2005, MNRAS, in Press
Johnston, S., Manchester, R. N., Lyne, A. G., et al. 1992, ApJ, 387, L37
Kramer, M., Xilouris, K. M., Lorimer, D. R., et al. 1998, ApJ, 501, 270
Levy, G. S., Sato, T., Seidel, B. L., et al. 1969, Science, 166, 596
Lommen, A. N., Kipphorn, R. A., Nice, D. J., et al. 2006, ApJ, 642, 1012
Lorimer, D. R., Yates, J. A., Lyne, A. G., & Gould, D. M. 1995, MNRAS, 273, 411
Manchester, R. N., Hobbs, G. B., Teoh, A., & Hobbs, M. 2005, AJ, 129, 1993
Mancuso, S. & Spangler, S. R. 2000, ApJ, 539, 480
Morris, D. J., Hobbs, G., Lyne, A. G., et al. 2002, MNRAS, 335, 275
Schatten, K. H. Wilcox, J. M. & Ness, N. F. 1969, Solar Phys., 6, 442
Splaver, E. M., Nice, D. J., Stairs, I. H., Lommen, A. N., & Backer, D. C. 2005, ApJ, 620, 405